Optical Filtering with Phase Singularities

William F. Ames, *REU program, College of William and Mary*
Irina Novikova, *College of William and Mary, Physics Department*

July 21, 2008

Abstract

I worked on constructing an optical filtering device to improve the data quality of Prof. Novikova's stored light experiment, which requires two beams, one much more powerful than the other, that exit the experiment nearly collinear such that standard filtering methods are not sufficient. I adapted the optical vortex coronagraph of Dr. Swartzlander of the University of Arizona for our experiment. The device takes advantage of the exotic properties of optical vortices, particularly their "doughnut" intensity pattern to suppress the unwanted beam without affecting the desired beam. Over the course of the REU program, I have worked on mathematical and computation modeling of the optical vortex coronagraph, and testing and improving the effectiveness of our prototype.

1. Introduction

The stored light experiment in the Quantum Optics lab at the College of William and Mary outputs two laser beams: the control field, which optically pumps the Rubidium cell, and the probe field, which is the beam carrying the data out of the experiment. The beams are of similar frequency and polarization, and come out of the experiment nearly collinear. Unfortunately, the control field is much more intense than the probe field, and the two are close enough that the two beams are nearly indistinguishable. Similar problems have long plagued astronomers, particularly in attempts to resolve the solar corona. The problem was solved by Bernard Ferdinand Lyot with the invention of the Lyot Coronagraph. Unfortunately, the Lyot coronagraph does not provide sufficient filtering for our problem, so we must resort to something else, specifically, the optical vortex coronagraph created by Grover Swartzlander, which uses the unique properties of optical vortex beams to achieve filtering not possible with the Lyot coronagraph. This paper details my efforts to build an optical vortex coronagraph to filter out the control field while minimizing attenuation to the control field.

2. Lyot Stop Coronagraph

The Lyot coronagraph was developed in the 1930s to directly view the sun's corona for the first time. A diagram of it can be seen below as Figure 1. The two beams enter at a small angle relative to each other from the left side of the diagram, going right. The first lens, L1, focuses both beams down to a point on the focal plane: FP1. On this focal plane there is some sort of occulting object: for a coronagraph meant to view the

sun, this would be a circular disk in the center, for our purposes, it would be an occulting mask designed to block one of the beams but not the other. A second lens, L2, of the same focal length as L1, is used to recollimate the outgoing beam. A third lens, labeled L3 in this diagram, could be placed in front of the beam to focus it onto a detector, though this is not necessary with our apparatus. A Lyot stop could be placed in front of this lens to reduce diffraction.

Figure 1: Coronagraph Diagram[1]

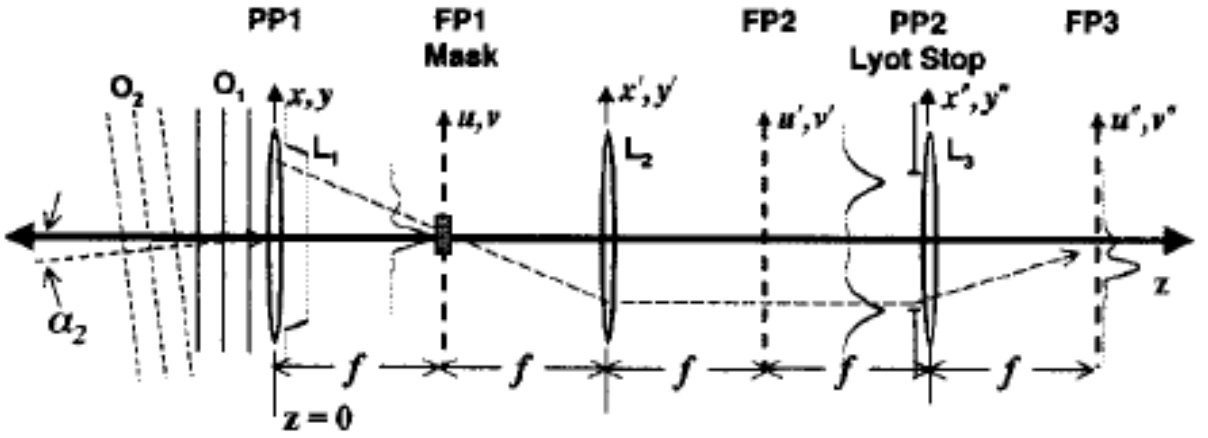

Unfortunately, the Lyot stop coronagraph is not sufficient for our application. The control and probe fields are so close together, that if the occulting mask were large enough to block out enough of the control field that the probe field would the visible, too much of the probe field would be lost. The control field is so much more powerful than the probe field that not blocking out nearly all of it would still drown out the probe field. Clearly, another solution is in order. That is why we have decided to build an optical vortex coronagraph.

3. Optical Vortices

Figure 2: Optical Vortex

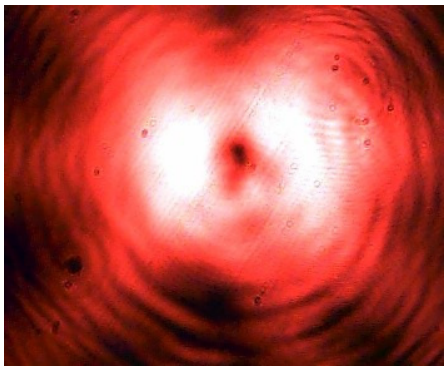

An optical vortex, is a zero of optical field, caused by destructive interference in a beam. An optical vortex beam has its field maximum in a donut shape around the vortex, instead of at the center of the beam, as shown in Figure 2. An optical vortex can be created in several different ways, the most important being with computer generated holograms and spiral phase plates. In a computer generated hologram, the interference pattern between an optical vortex beam and a Gaussian beam is calculated, and the results printed onto a hologram. The second method is the spiral phase plate: a piece of glass is cut in steps in a circular pattern, with each step being incrementally thicker than the one before it, until it reached the beginning, where there is a discontinuity. The total phase shift across the circumference of the phase plate should be 2π times the wavelength. The number of $2\pi\lambda$ phase shifts around the circumference of the phase plate is referred to as the topological charge, m. See Figure 4 for a picture of an optical vortex spiral phase plate. It is a spiral phase plate similar to the one shown which is used to create the optical vortex used in the optical vortex coronagraph. It is the center of the phase plate: the point where all the stair-step pieces join together, that is what creates the vortex. A beam which passes through the phase plate without passing through that center point will not become an optical vortex beam. The optical vortex beams we use are Laguerre-Gaussian beams, which are of the form of Equation 1.

Figure 3: Gaussian Beam

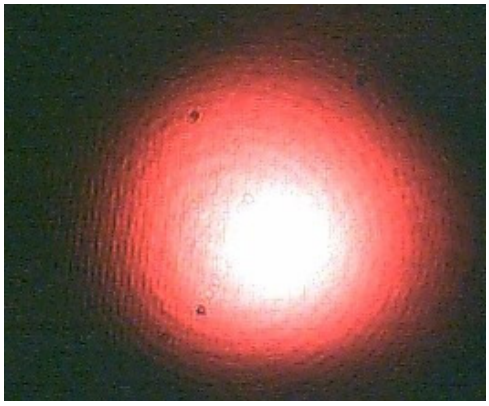

Figure 4: Vortex Phase Mask, available: http://www.u.arizona.edu/~grovers/ov

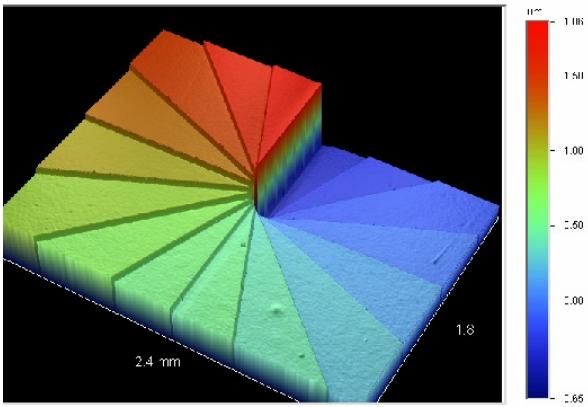

$$E = \left(\frac{r}{w_0}\right)^m e^{-r^2/w_0^2} e^{im\vartheta} e^{ikz - i\omega t}$$

(Equation 1)

Where w_0 is a parameter representing the width of the beam, t is time, and r, φ, and z are the cylindrical coordinates, and m, the topological charge. For comparison, a Gaussian beam is shown in Equation 2.

$$E(r,z) = E_0 \frac{w_0}{w(z)} e^{-r^2/w(z)^2} e^{-i(kz - \arctan(z/z_R) + kr^2/(2R(z)))} \qquad \text{(Equation 2)}$$

Where w(z) is a function defining variations in beam waste, z_R is the Rayleigh length and is equal to pi times the beam waist width squared over the wavelength, and $R(z)=z[1+(z_R/z)^2]$.

4. Optical Vortex Coronagraph

The optical vortex coronagraph is similar to the Lyot stop coronagraph. Instead of using and occulting mask to block one of the beams on the plane FP1 (see Figure 1) an optical vortex phase plate is placed in the focal plane such that the unwanted control field becomes an unwanted optical vortex beam, while the desired beam, the probe beam, goes through the phase plate unaltered. The two fields are then recollimated upon arrival at the second lens. A pinhole smaller than the vortex is used to block the vortex beam, while the probe field goes right through the pinhole. In principle, this allows for complete elimination of the control field without affecting the probe field. The optical vortex coronagraph was first proposed and constructed by Dr. Grover Swartzlander at the University of Arizona for the detection of extrasolar planets.[1]

5. Design and Construction of the Optical Vortex Coronagraph

The construction of the prototype optical vortex coronagraph proceeded in three stages. A diagram of the current apparatus can be seen below as Figure 5. The first stage, completed during the school year, consists of the ersatz control field laser, the lenses which focus the light on the phase mask and recollimate it afterwards, the phase mask itself, and the pinhole. The pinhole is easily removable, and the optical vortex phase mask is mounted on a translation stage so that the vortex can easily be turned on and off. Originally, at the end of the apparatus, after the pinhole, was a

Figure 5: Apparatus Layout

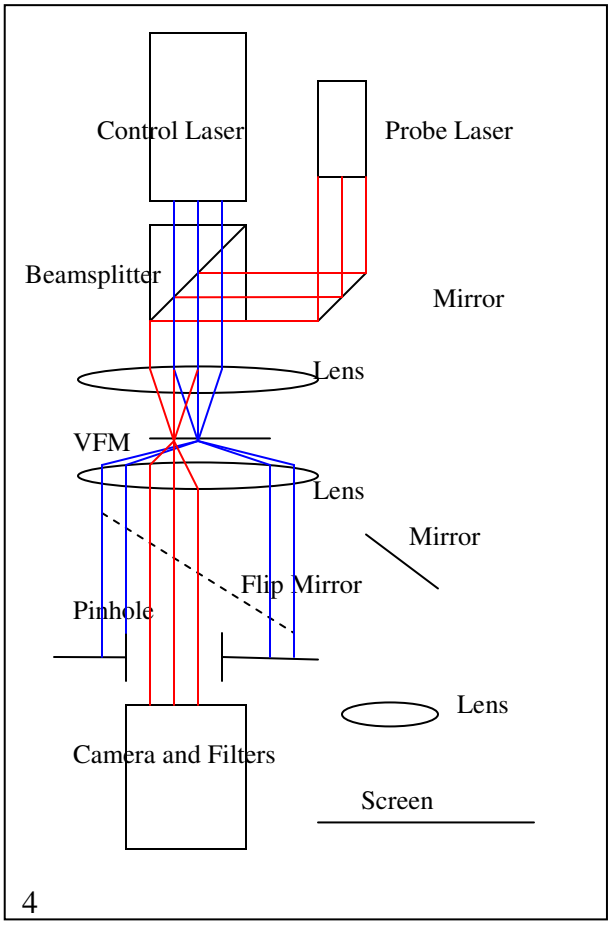

lens used to project the image on to the back wall. Briefly, a photodiode was placed at the end, which was, at the beginning of the summer, replaced with the beam imaging camera and filters which are there now. The second stage was the addition of the flip mirror and a normal mirror which allow me to project the vortex on the wall, to easily check to make sure I have one, without removing the camera. The final stage of the coronagraph vortex thus far is the addition of the ersatz probe laser, a mirror, and a polarizing beam splitter, which are used to create the fake probe field and provide it with a small angle relative to the control field. Due to a lack of a rotary stage, the exact angle is unknown; it must be determined by eye.

6. Measuring the Effects of Diffraction

With my attempts at calculating the ideal size for the pinhole stymied, I resorted to an experimental solution. First, I set up the beam imaging system developed by one of our graduate students, Matthew Simons. It consists of a modified web camera, really just a CCD camera, along with appropriate software: PhotoImpression 3 to take the pictures, and ImageJ for data analysis. Using this system, I took 3 pictures of the vortex without

	First Alignment		Second Alignment		Third Alignment	
	Pinhole	No Pinhole	Pinhole	No Pinhole	Pinhole	No Pinhole
Vertical Profile	54	252	83	261	83	225
Horizontal Profile	83	261	128	239	75	167
Upper Left-Lower Right Profile	90	279	81	255	85	180
Upper Right-Lower Left Profile	90	225	74	247	88	222
Average	79.25	254.25	91.5	250.5	82.75	198.5

Effective Vortex Size Factor, First Alignment	Effective Vortex Size Factor, Second Alignment	Effective Vortex Size Factor, Third Alignemnt
3.2	2.7	2.3

Average Effective Vortex Size Factor
2.8

the pinhole in place, and 3 pictures with the pinhole in place. The images come in pairs, one with the pinhole in place, one with it removed. I would then unalign the vortex phase mask, and realign it and replace the pinhole for the next pair. Using ImageJ, took four profiles of each vortex: one vertical, one horizontal, and the other two at 45 degree angles to the others, all intersecting at the center of the vortex. I transferred the data on the beam profiles into Excel, where I re-graphed them and recorded the full-width-half-max of each vortex profile. I then averaged together each of these vortex width measurements

for each vortex, and found the ratio between pinhole and non-pinhole vortex size. The results can be seen summarized in Table 1.

Table 1: Effect of Diffraction on Effective Vortex Size, Measured in Micrometers

Looking at this data, the diagonal profiles seemed to behave a touch strangely, so I decided not to use diagonal profiles again. I think this is due to aliasing: the line is jagged, and the jump from pixel to pixel can carry one across a curved boundary region multiple times. The data clearly indicated a reduction in effective vortex size due to diffraction. I decided to see how this would change with different sizes of vortex. To take data on this, I took a series of pictures with a lens placed before the pinhole to change the size of the vortex. The first lens used had a 50mm focal length, and was placed 14 cm before the pinhole, with the pinhole 9.5 cm from the camera. Next, I did a series of pictures with the lens 13 cm from the pinhole and the pinhole 8.5 cm from the camera. Finally, I took a series of pictures with the lens 3 cm from the pinhole and the pinhole 8 cm from the camera. I did no formal data analysis on these pictures, as it became clear that the vortex was effectively destroyed: diffraction patterns were clearly visible all the way inside the vortex, and there was frequently a bright spot: Poisson's Spot, dead center in the vortex, at the theoretically darkest point. Clearly, the diffraction of the optical vortex is a serious problem for the coronagraph, capable of completely ruining its operation.

7. Characterization of Complete Optical Vortex Coronagraph Prototype

Figure 6: Control and Probe Fields Pre-Filtering

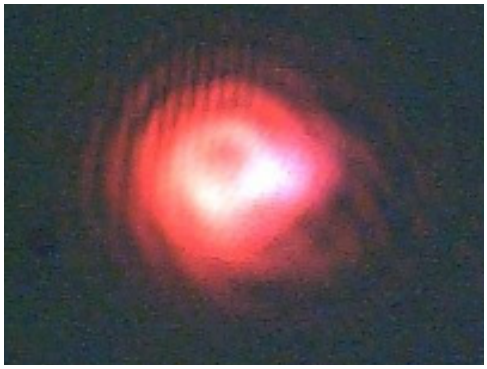

After adding the laser to represent the probe beam and the beam splitter to allow me to control the angle between the two, I began work on the characterization of the prototype filter. I did this by taking a series of photographs, one of the probe field and vortex with the pinhole in place, a second with the vortex and the pinhole, a third with the probe and the pinhole, a picture of the control field without the vortex, the probe field, and the pinhole, the same thing with no pinhole, the probe field with no pinhole, and the vortex-less control field with no pinhole. Figure 6 shows the system with no filtering whatsoever. The control and probe fields are indistinguishable. Figure 7 shows the results after filtering: while the control field is still present, it is much fainter, and it and the probe field are clearly distinguishable. Using ImageJ's ability to subtract one picture from another, I created images of the light filtered by the vortex coronagraph, the light filtered by the coronagraph without the vortex, the probe light filtered out by the vortex coronagraph, and the control field light filtered out by the vortex coronagraph. I analyzed this data in two different, similar ways. In both cases, I used ImageJ to add up the total amount of light in a circle encompassing the

beam on the picture: it produces an average light level over an area, and the area of the selection. I then multiply these two values together. To control for the fact that the camera does collect a significant amount of light in the black regions, I then select a small circle of black in a corner, and get the same statistics. I then multiply the average pixel value in the black region by the area of the region of interest, and subtract that from the total amount of light in the region of interest. The results of this method can be seen in Table 2. The second method was the same, only I took a picture of the darkness, with no lasers on, and subtracted it from each picture before doing the data analysis. These results can be seen in Table 3. As can be seen, at the moment the prototype filter is capable of filtering out ~80% of the control field, while leaving about two-thirds of the probe field intact. I tested the reliability of both of these methods by comparing the values found using different sizes of circle around the regions on interest, and found that all of the numbers in the data are accurate to 20%.

Figure 7: Control and Probe Fields Post-Filtering

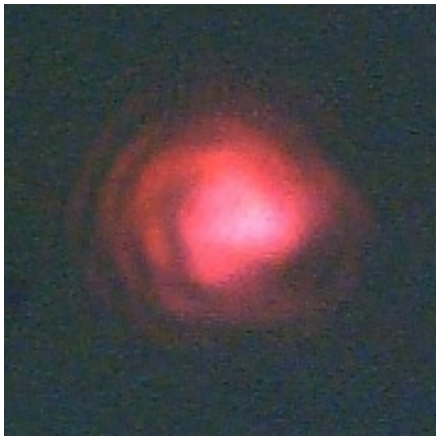

Table 2: Prototype Filter Testing, without black subtraction

Image	Post-Filtering Control	Post-Filtering Probe	Pre-Filtering Probe	Pre-Filtering Control
Illuminated Area	14214	10005	12380	30795
Illuminated Mean	65.119	75.492	76.317	84.105
Dark Mean	51.155	51.533	47.451	46.879
Total Illumination	925601.5	755297.46	944804.46	2590013.475
Total Illumination-Dark Control	**198484**	**239709**	**357361**	**1146374**
Control Filtering Ratio:	5.8			
Probe Filtering Ratio:	1.5			

Table 3: Prototype Filter Testing, with black subtraction

Image	Post-Filtering Control	Post-Filtering Probe	Pre-Filtering Probe	Pre-Filtering Control
Illuminated Area	10504	6434	11030	33798
Illuminated Mean	38.384	56.708	47.508	48.567
Dark Area	3125	2299	2778	2252
Dark Mean	15.61	15.944	12.117	11.757
Total Illumination	403185.536	364859.3	524013.2	1641467
Total Illumination-Dark Control	**239218**	**262275**	**390362**	**1244104**
Control Filtering Factor:	5.2			
Probe Filtering Factor:	1.5			

I also needed to determine what the best size for a new pinhole would be. I took a series of pictures of vortices, and averaged together several of their profiles to produce an average vortex profile. I then did the same thing with a several profiles of a probe field picture. I then found the distance between the two points where the average probe and average control fields are equal, and found it to be approximately 500 micrometers. Clearly, however, the diffraction through the pinhole was causing a serious problem, most likely because a pinhole exactly the same size of the usable portion of the vortex is nearly impossible to align perfectly. As a consequence, we elected to purchase a new, 150 micrometer pinhole.

8. Modeling of Optical Vortices

The main objective for the summer was to calculate the ideal pinhole size, determine why second order vortices are the best for filtering, and to develop a system to model the behavior of the apparatus without having to redo alignments or add/remove components. The program was to be based on a LabView program written by a graduate student here: Kelly Kluttz. The LabView code modeled a sort of generalized Schlieren effect. The Schlieren effect is used to turn phase variances into intensity variances, so that they can be easily detected. I installed the program on the computer in the lab, and got help from Kelly Kluttz in learning to use it and how it works. The program models a beam passing through an arbitrary phase distribution, then through a lens, another arbitrary phase distribution at the focus of the lens, and another lens to recollimate the beam. One gives the program the initial phase distribution and the focal plane phase distribution, and the program produces what one would see on a screen behind the last lens. I then tried to see what would happen if I gave it a vortex phase mask as the initial phase distribution, which is similar to the situation in the coronagraph. I painstakingly drew it out in Paint, with the colors along the grayscale indicating a phase change from 0 to 2π. The results, shown as Figures 8 and 9 were impressive, it even seemed to have some of the same defects as the real vortex. I then proceeded to develop a faster and more powerful way to insert phase masks into the LabView program. First, I find a

Figure 8: Input phase mask for LabView

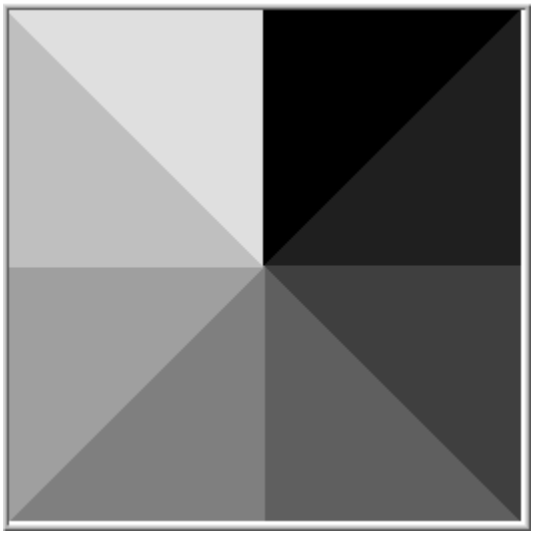

Figure 9: Output of LabView beam modeling

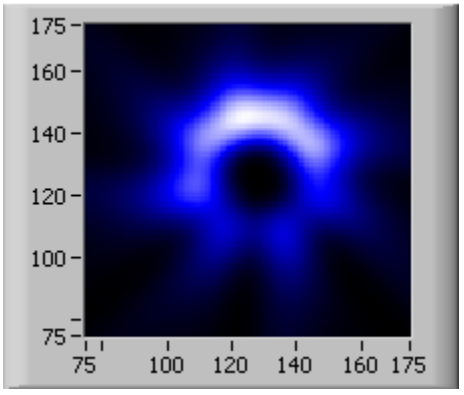

mathematical way to model the phase mask I want, and generate the phase mask in MatLab using the three-dimensional graphing function, which I then convert to a scaled image. I turn off the axes, convert it to black and white, and save the resulting image in JPEG format. I then load the image into GIMP, where I change the resolution to 150 by 150, the resolution the LabView program needs, and change the image size to 256 by 256, also a requirement of the program. I then change the image to grayscale in GIMP, center the image, and save it as a BITMAP.

The next objective was to modify the LabView program to include the pinhole. This would allow us to completely model the effects of our apparatus on the optical vortex beam. In the more short-term, it would also assist in determining what size of pinhole we needed, since we knew the 500 micrometer one to be too large. This would require adding an amplitude distribution at the end of the current program, as well as calculating the diffraction through the pinhole.

There are two approximations used in calculating diffraction, the Fresnel, or near-field, and the Fraunhofer, or far-field. As a rule, the far-field approximation can be used when the Fresnel number is much less then one, where the Fresnel number, F, is described by Equation 2.

$$F = \frac{a^2}{L\lambda} \qquad \text{(Equation 2)}$$

Where a is the size of the aperture, L is the distance from the aperture to the screen/detector, and λ is the wavelength. For all probable designs of the filter, aperture size is on the order of hundreds of micrometers, distance between the aperture and the detector is on the order of centimeters, and wavelength is in hundreds of nanometers, so clearly F<<1, and the Fraunhofer approximation can be used.

The Fraunhofer diffraction equation outputs a function in terms of position on the image plane, when given a function in terms of position on the diffracting aperture plane. The equation looks like this:

$$U(x,y) = \frac{e^{ikz} e^{i\frac{k}{2z}(x^2+y^2)}}{i\lambda z} \iint U(\xi,\eta) e^{-i\frac{2\pi}{\lambda z}(x\xi+y\eta)} d\xi d\eta \qquad \text{(Equation 3)}$$

Where x and y are position on the image plane, ξ and η are position on the aperture plane, and z is the distance between the two planes. U(ξ,η) is the distribution at the plane of the aperture. The integration is performed across the surface of the aperture. Converting the aperture plane coordinates into polar coordinates r and φ, this results in the following equation in the case of a Laguerre-Gaussian beam:

$$U(x,y) = \frac{e^{ikz} e^{i\frac{k}{2z}(x^2+y^2)}}{i\lambda z} \iint \left(\frac{r}{w_0}\right)^m e^{-r^2/w_0^2} e^{im\vartheta} e^{ikz-i\omega t} e^{i\frac{2\pi}{\lambda z}(xr\cos\vartheta + yr\sin\vartheta)} r dr d\vartheta \qquad \text{(Equation 4)}$$

Unfortunately, actually solving this integral is quite difficult, in fact, it is analytically impossible. Numerical integration routines do not converge. In response, I tried several approximations of this integral. The first, a pair of Taylor series, one in r and the other in φ, were horrible approximations of the actual function. In response, I broke up the r-portion into 10 different areas, did a Taylor series about each of these segments, and created a piecwise function which was an excellent approximation of the amplitude distribution. To deal with the rest of the function, I tried to construct a Fourier series in terms of φ, but that could not be calculated in reasonable time. Out of ideas, I put these calculations on hold.

9. Alternative Optical Vortex Coronagraph Design

I have also designed another version of the optical vortex coronagraph, in which the probe field becomes the optical vortex, and the control field remains the Gaussian beam. The design for the prototype is shown as Figure 10. Up until the phase mask, it is exactly the same as the normal optical vortex coronagraph. This time, it is the probe field, instead of the control field, that becomes an optical vortex. Instead of a pinhole filtering out the vortex, it uses an occulting mask in the center of the vortex to filter out the Gaussian beam, while the vortex passes around it. It then uses a lens to focus the vortex down onto a second vortex phase mask to turn it back into a Gaussian beam. Another lens then collimates the beam before sending it to the camera. The primary advantage of this system is that the problems of diffraction around the occulting mask are well understood and have already been solved. While we only have one phase mask, it has multiple vortex-creating elements on it so we could use mirrors to send the vortex back through one of the other vortex elements. This was not shown on the diagram for the sake of simplicity and legibility.

Figure 10: Alternative Filter Design

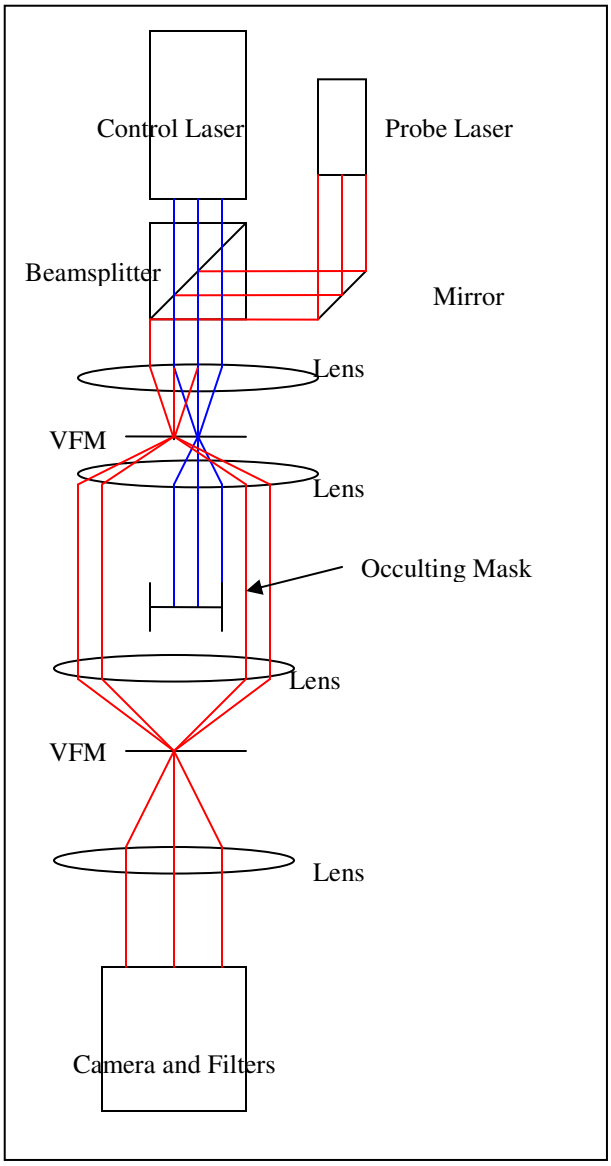

10. Conclusions

Based on my work this summer, I can conclude that the important part of the optical vortex phase mask is the center, and that so long as the center is precisely machined, imperfections in the rest are more or less irrelevant. While Nate Wright has since found a way to make the diffraction integrals numerically solvable, it remains clear that a LabView program capable of doing the modeling we had hoped would be at best extremely difficult to produce. Diffraction of the vortex through the pinhole is a serious problem, which would probably best be addressed through the use of a smaller pinhole. Even with the current pinhole, the prototype filter is still doing a reasonable filtering job, which would probably be dramatically improved by the use of another pinhole. I also found my method of analyzing my images to be precise enough to be useful, but not exceptionally reliable.

11. Selected References

1. Gregory Foo, David M. Palacios, and Grover A. Swartzlander, Jr**,**
"Optical vortex coronagraph"
Opt. Lett. **30**, 3308-3310 (2005)

2. Z.S. Sacks, D. Rozas, and G.A. Swartzlander, Jr.,
"Holographic Formation of Optical-Vortex Filaments"
J. Opt. Soc. Am. B, **15**, 2226-2234 (1998)

3. Zhongyi Guo, Shiliang Qu, and Shutian Liu,
Generating optical vortex with computer-generated hologram fabricated inside glass by femtosecond laser pulses
Opt. Commun. **273** p. 286 (2006),

4. David M. Palacios
An Optical Vortex Coherence Filter
2004, Available at:
http://www.wpi.edu/Pubs/ETD/Available/etd-0824104-123434/unrestricted/palacios.pdf